Thermophysical Properties of ESR-Electrofluxes (Part 1: Density)

Semiramis Akbari[1], Jan Reitz[1], Bernd Friedrich[1]
[1]IME Process Metallurgy and Metal Recycling, RWTH Aachen University
Intzestraße 3, 52056 Aachen, Germany

Keywords: Electroflux, Density, physical properties, FactSage, thermal properties

Abstract

Process optimisation for electroslag remelting (ESR) is nowadays based on numerical simulation of the process which depends on accurate knowledge on properties of the liquid phases modelled. For the commonly applied ESR Fluxes in the system CaF_2-CaO-Al_2O_3, the density, surface tension, viscosity and electrical conductivity are presently investigated. This publication is dedicated to the measurement of density as a function of temperature and CaF_2 content, based on the Archimedes method. Measurements are supported by FactSage® calculations and DTA measurements for determination of heat capacity, melting enthalpy, solidus and liquidus temperature.

Introduction

The electroslag remelting (ESR) process has secured its place among different remelting processes [1] and is now widely used for the production of defect-free ingots of high-performance alloys for the manufacturing of components in aerospace and land-based turbines [2]. The quality of ESR ingots is significantly higher than that of air-melted and conventionally cast ingots [3]. The selection of an appropriate flux or flux system is essential for the success of the remelting operation. The choice of flux is governed by physical and chemical considerations. The process generally is one of oxidation; hence, precautions are necessary to minimize the oxidation losses of alloying elements with high free energies of oxide formation (e.g., silicon, aluminium and titanium). The flux provides the source of heat because of its resistivity and controls the compositions of the remelted alloy [4]. All ESR fluxes contain CaF_2 as the primary constituent. Oxides may be added to the flux to raise the resistivity (as to make melting more efficient electrically) or to modify the flux chemistry with regard to its reactivity with the metal being melted [2].

The fluxes are usually liquids in the system CaF_2 + CaO + Al_2O_3 and range widely in composition. Sometimes additions of SiO_2, TiO_2, and MgO are used. In general, CaF_2-based fluxes are chosen with additions of Al_2O_3 and CaO to increase the resistivity and promote sulphur removal, respectively [5]. Alkali metal oxides and transition element oxides are to be avoided. Maximum desulphurization is achieved with fluxes of basicity higher than 5. Care must be taken in using fluxes to ensure the absence of unwanted trace elements that would transfer to the ingot during ESR. Impurity levels may require further restriction for certain alloy grades if high purity in the alloy is to be maintained. Fluxes without CaF_2 may be employed although their use on an industrial scale has been very limited. The existing ESR operations are under continuous improvement through process optimisation due to ever increasing requirements on material quality and homogeneity. Several of the improvement approaches directed towards numerical simulation of the process and computational algorithms have achieved a suitable stage of development. Yet these calculations depend tremendously on accurate thermophysical data of the liquid phases. These data are not always known; empirical factors are applied in order to adjust assumptions or values reported in literature linking numerical data into accordance with experimental validation. In order to reach another step in process optimisation, research at IME is aiming at the investigation of thermophysical properties in salt, flux and flux systems such as Electrofluxes due to the highly important role of properties such as density, electrical conductivity and viscosity on the behaviour of Electrofluxes in the ESR process.

Methodology of Thermophysical Properties Measurement – Density

The exact knowledge of the density at operating temperature is necessary to analyse processes and properties, e.g. phase separation, viscosity, surface tension or thermal expansion [6]. Different techniques of density measurement at high temperatures are available e.g. the Archimedes, the dilatometry and the pyknometer method. The Archimedes method, used in this study is based on the principle that the volume immersed in a fluid is equal to the weight of displaced fluid and is applicable to high temperatures (>1000°C) as well as to corrosive melts. The density under Archimedes method will be calculated through the following equations:

$$\rho_m - \rho_a = (m_a - m_m)/V\,(1+\varepsilon)^3 \qquad (1)$$

Where ρ_m and ρ_a are the densities of melt and air, m_a and m_m the weight of the measuring probe in air and melt, V is the volume of the probe at the related temperature and ε is the linear thermal expansion coefficient of the probe. In the case of elementary or binary salt mixtures, the density measurement has been frequently investigated [7-9], but ternary or quaternary mixtures very seldom. The "Archimedes" measurement instrument consists of a hydrostatic balance and a free hanging probe. The weight of this probe is weighed initially in air, and afterwards inside the melt. In figure 1 the principle of this method is illustrated schematically [6]. Trials were conducted in a fully evacuated and Ar-flushed device using probes, wire and clasp made from Mo or W-10Rh. In order to calculate the density of a liquid, the exact volume of the measuring probe is required, in our case the geometrically determined volume is converted to the weight divided by density of the sample material, which can be taken from literature as function of temperature. For example, the polynominal definition of Mo density is represented by following equation [10]:

$$\rho_{Mo} = -3.66E\text{-}08\ T^2 - 0.000157\ T + 10.27 \qquad (2)$$

Figure 1 illustrates the chamber used in the density measurement furnace. An "Alsint" (99.7% Al_2O_3) crucible, a one-sided closed tube with dimensions of 11×86×440 mm build the insulating wall. A stainless steel lid equipped with water cooling as well as with an Argon injection system served for a controlled atmosphere inside the tube. The slag is put into a glassy-carbon crucible at the bottom of the Al_2O_3 tube. The ESR-fluxes investigated contain mostly CaF_2, CaO, Al_2O_3 and MgO as the main components, as well as some quantities of SiO_2, TiO_2, FeO and traces of C, P, S, Bi and Pb, which are not considered. Some fluxes contain less or no CaF_2. Table I shows the compositions of the electrofluxes before and after the experimental trials.

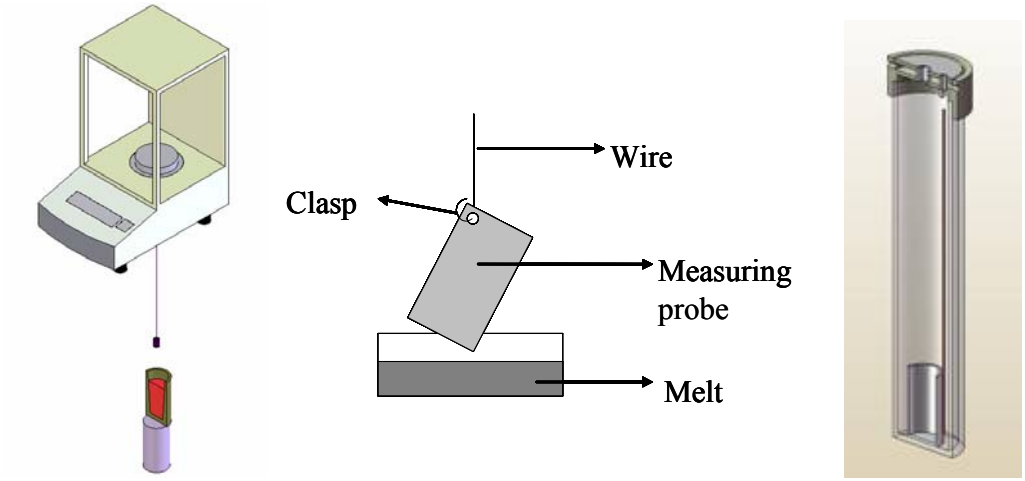

Figure 1: Scheme of the "Archimedes" density measurement device and the applied principle [6] as well as a cross section of the new construction of furnace chamber (right)

These analyses were carried out through X-ray fluorescence analysing (XFA) as well as calibration via those methods, in which Ca-content was investigated independently such as dissociation and titration. The contents in table I has been normalized to 100%.

Table I: Chemical composition of electrofluxes applied in density measurements (wt %)

Flux Nr.	Analyse	FeO	V_2O_5	TiO_2	CaO	SiO_2	Al_2O_3	MgO	CaF_2	P	C	S	Σ
1	After	0,02%	0,01%	0,01%	29,95%	1,22%	33,66%	2,78%	32,26%	0,00%	0,08%	0,01%	100,000%
	Before	0,11%	0,01%	0,01%	28,50%	1,57%	32,37%	3,46%	33,95%	0,01%	0,01%	0,01%	100,00%
2	After	0,01%	0,01%	0,01%	12,29%	0,83%	21,97%	2,00%	62,83%	0,00%	0,05%	0,01%	100,00%
	Before	0,04%	0,01%	0,01%	15,10%	0,92%	23,20%	2,20%	58,50%	0,00%	0,01%	0,01%	100,00%
3	After	0,01%	0,01%	0,01%	15,73%	0,25%	14,33%	1,10%	68,34%	0,00%	0,19%	0,02%	100,00%
	Before	0,05%	0,01%	0,01%	16,19%	0,29%	15,04%	1,34%	67,03%	0,01%	0,01%	0,02%	100,00%
4	After	0,02%	0,01%	0,01%	17,98%	0,30%	21,97%	1,20%	58,23%	0,00%	0,27%	0,01%	100,00%
	Before	0,07%	0,01%	0,01%	17,47%	0,41%	20,24%	1,51%	60,25%	0,00%	0,01%	0,01%	100,00%
4a	After	0,01%	0,01%	0,01%	13,49%	0,30%	16,09%	7,80%	62,07%	0,00%	0,19%	0,02%	100,00%
	Before	0,10%			13,46%	0,42%	17,44%	7,41%	61,13%	0,01%	0,01%	0,02%	100,00%
5	After	0,01%			0,60%	0,15%	0,17%		99,03%	0,00%	0,03%	0,01%	100,00%
	Before	0,01%			0,97%	0,19%	0,03%		98,78%	0,00%	0,01%	0,02%	100,00%
6	After	0,04%	0,01%	2,20%	18,52%	0,29%	21,63%	4,41%	52,76%	0,00%	0,13%	0,01%	100,00%
	Before	0,10%	0,03%	3,06%	19,60%	0,32%	21,45%	5,20%	50,21%	0,01%	0,01%	0,01%	100,00%
7	After	0,05%	0,02%	0,02%	25,92%	0,26%	18,99%	2,81%	51,64%	0,00%	0,27%	0,01%	100,00%
	Before	0,09%	0,02%	0,02%	28,12%	0,31%	19,83%	2,97%	48,61%	0,00%	0,01%	0,01%	100,00%
8	After	0,04%	0,01%	0,01%	29,02%	0,22%	30,12%	2,01%	38,36%	0,00%	0,20%	0,01%	100,00%
	Before	0,09%	0,01%	0,01%	26,35%	0,27%	30,77%	2,75%	39,73%	0,01%	0,01%	0,01%	100,00%
9	After	0,07%	0,01%	0,01%	39,22%	1,24%	41,93%	4,42%	13,07%	0,00%	0,02%	0,01%	100,00%
	Before	0,14%	0,01%	0,01%	38,11%	1,71%	40,60%	4,31%	15,10%	0,01%	0,01%	0,01%	100,00%
10	After	0,03%	0,02%	0,03%	28,90%	0,53%	28,90%	0,77%	40,61%	0,00%	0,19%	0,02%	100,00%
	Before	0,10%		0,02%	29,43%	0,19%	30,61%	0,61%	39,02%	0,01%	0,01%	0,01%	100,00%
11	After	0,01%	0,01%	0,02%	20,88%	21,88%	0,60%	11,39%	45,15%	0,00%	0,06%	0,01%	100,00%
	Before	0,15%		0,01%	20,85%	21,66%	0,14%	11,41%	45,75%	0,01%	0,01%	0,01%	100,00%
12	After	0,05%	0,01%	0,03%	47,62%	0,46%	46,09%	5,61%		0,01%	0,11%	0,01%	100,00%
	Before	0,11%	0,01%	0,03%	48,16%	0,39%	46,45%	4,84%		0,01%	0,01%	0,01%	100,00%

Methodology of FactSage® calculations for determination of thermal properties

Databases, selected phases, restrictions and parameters in FactSage® calculations

For the experiments, as well as for process optimisation in ESR, an estimation of solidus temperature T_{sol}, liquidus temperature T_{liq}, enthalpy/heat of melting H_m and heat capacity C_p in solid, liquid and semi-solid state are of high interest. These calculations are supported by thermal analysis via DTA/TG. Occurring phases where examined carefully in order to enhance the understanding of the observed flux systems in terms of compositions, occurring phase transformations and behaviour during melting. The database Fact53 is the present standard database delivered with FactSage® 5.5 [1] for thermochemical data of pure substances, while FTOxide includes pure substance data and solution models for oxide solutions like the fluxes under examination in this programme. All pure solid oxides and halides were allowed, while metals and intermetallics were suppressed. “Duplicates” were eliminated by giving priority to the data from FTOxide which also incorporates the solution model. Liquid oxides were not allowed as they are assumed to dissolve in the liquid solution phase. SLAGA was selected for modelling the liquid solution of the incorporated oxides and CaF_2 as the only occurring non-oxide component. Solid solutions SPINEL and AMONOXIDE (Wüstite) were allowed to test the thermochemical occurrence of these solutions against the corresponding stoichiometric pure substances (e.g. Spinel types) but were only observed in minor quantities. This is in accordance with FactSage® documentation. A possible two phase immiscibility in case of “higher” CaO content is taken into account for by setting the I-option on SLAGA as a standard. Gas phases were not selected in order to avoid the effects of evaporation on the calculation of heat of melting and variations in composition due to evaporation effects. It has to be pointed out, that the FTOxide’s solution model for the liquid flux phase SLAGA is only approved experimentally for dilute solutions (<10%) of CaF_2 in an oxide-based flux.

Therefore, all of the examined slags are based on extrapolated calculations of activity coefficients and could be less accurate with increasing CaF_2 contents. Because experimental determi-

nation of thermal properties was conducted in parallel, these restrictions were accepted and carefully considered for the present case.

Results and Discussion

Calculated Solidus and Liquidus Temperatures of Electrofluxes

As it can be observed in Figure 2, a small amount of liquid flux phase appears to be physically present at roughly 1050°C, yet, this phase represents < 10% of the total system mass. From a practical standpoint, the flux would appear to be solid at these temperatures with the liquid phase being entrapped inside a solid grain structure. At roughly 1250°C, when a $Ca_3MgAl_4O_{10}$ phase melts, the mass fraction of liquid SLAGA approaches 50%. At 1414°C excess solid CaF_2 melts and results in a system with less than 10% solids, which appears to be liquid from a practical point of view. This fraction of $Ca_5Ti_4O_{13}$ should be stable up to 1800°C. In industrial practice, intensive stirring of the ESR flux occurs, resulting in the fact that the presence of such a small solid quantity should have no effects on the process. In our opinion it should be discussed if liquidus and solidus temperatures, applied in their strictest sense give wrong indications for the determination of e.g. the enthalpy of melting, the semi-solid range and comparison of different flux compositions in experimental practice (e.g. by DTA).

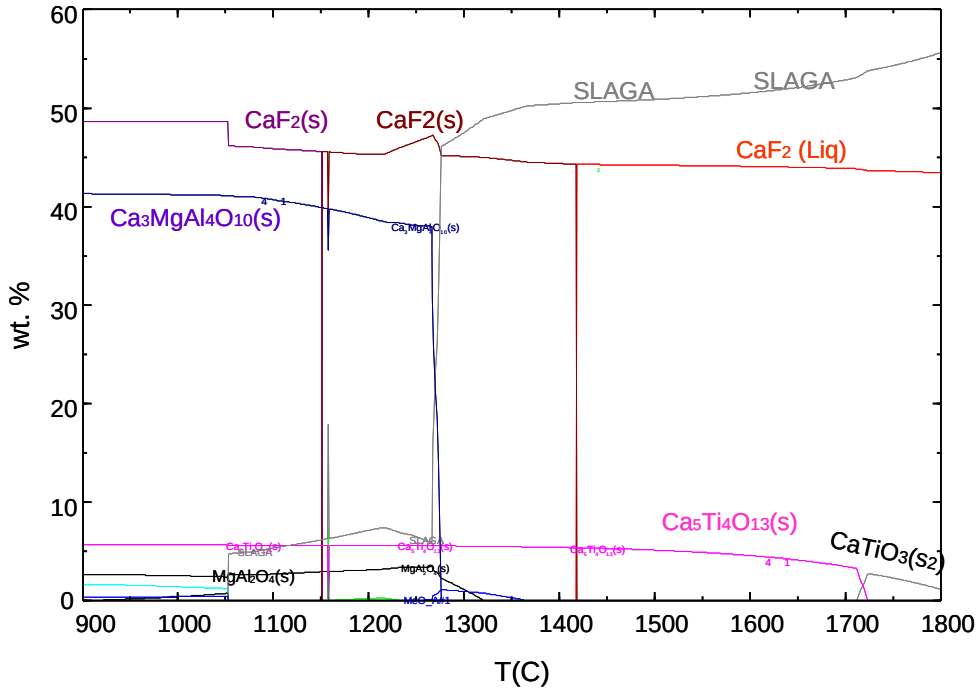

Figure 2: weight proportion calculation of electroflux Nr. 6 showing the existence of a solid phase of $Ca_5Ti_4O_{13}$ up to higher temperatures

It is therefore proposed to adjust these values by application of a 10 wt % margin in the sense that T^*_{sol} corresponds to the temperature where more than 10 % of liquid phase appear to be in the system. Vice-versa, T^*_{liq} should be defined as the temperature where less than 10% of the system is still solid. With these modifications, the liquidus and solidus values determined by FactSage® calculation are presented in figure 3. According to the databases pure fluorspar shows a melting temperature (in this case liquidus) of about 1414°C. Figure 3 shows that the solidus temperature of most of fluxes could be determined to be at approx. ±1000°C and 100% liquid phase (liquidus temperature) is achieved for some fluxes (Nr. 2, 7, 8, 9 and 11) at about 1400 °C

(the same as pure CaF_2) and for some of them quite higher than 1400 °C. According to table I, electrofluxes Nr. 2, 7 and 11 are containing ca. 50 wt % CaF_2 as well as ca. 20 Wt % Al_2O_3, over 15 Wt % CaO and ca. 20 Wt % SiO_2 (in the case of flux Nr. 11). In spite of existence of the above mentioned oxidic components, which have normally higher melting temperature than pure CaF_2, the liquidus of these fluxes is quite similar to pure fluorspar.

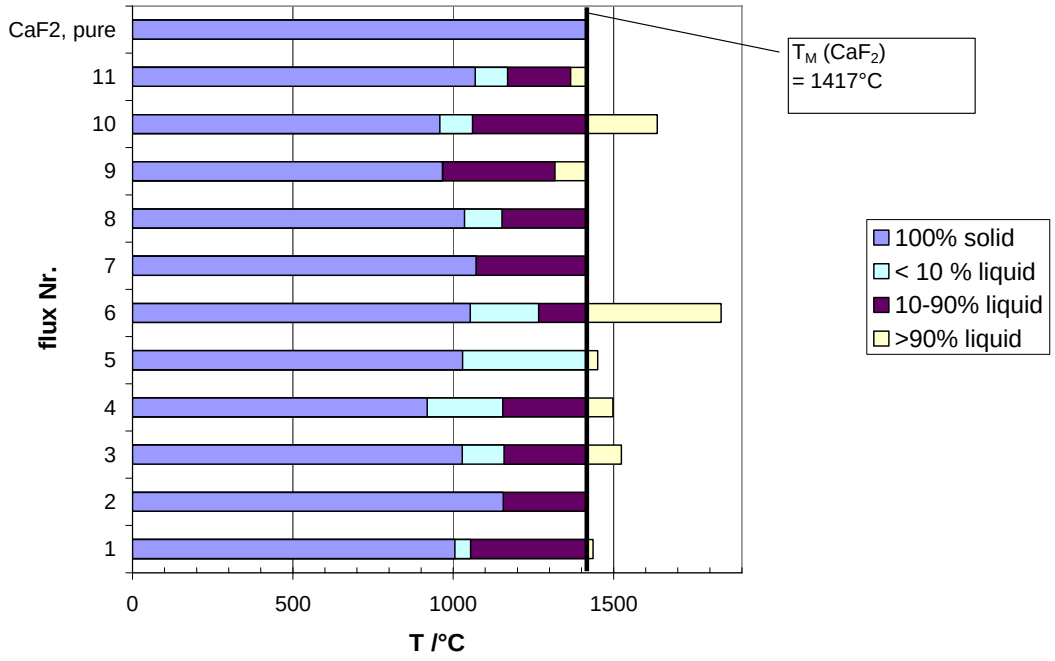

Figure 3: Melting point ranges calculated through FactSage®

Density Measurements

According to figure 3, the temperatures established in density measurement experiments were set to 1500, 1550 and 1600°C for most electrofluxes and 1540, 1570 and 1600°C for those with higher than 1500°C liquidus temperatures. Figure 4 illustrates the density values versus the content of CaF_2. It shows that an electroflux containing 14.5 wt% of fluorspar has the highest density and the queue proves an expected order with a rising value of calcium fluoride. Those fluxes containing quite similar amounts of CaF_2 have density values rather close to each other, although the mass ratios of $CaO:Al_2O_3$ are different. Furthermore, the density values of all electrofluxes decrease at rising temperatures. This fact confirms the CaF_2 content is the main factor in comparison with other components.

Two electrofluxes (Nr. 9 and 6) have been compared with results delivered from literature, here by Ogino [11], Zhmoidin [12] and Sikora [13]. The exact chemical composition of fluxes studied in this paper has of course not been found in other references, but it has been tried to select those publications, whose experiments have been done with quite similar compositions; at least in the case of the main components. It was found that their results differ rather significantly, which shows the complexity of density measurement in these fluxes and that different methodologies lead to quite different results. Nevertheless the density values measured in this work (based on experiment repetitions) are very close to the findings of Zhmoidin. However, according to what was discussed in the previous chapter, there is a possibility of existing “not-melted” particles for some electrofluxes even up to 1600-1800°C (see fig. 3). This could lead to inaccurate measurements, as these solid particles influence the measurements through sticking to the measuring probe. That may be one reason for different findings of authors.

Additionally, the ternary diagram of CaF_2-CaO-Al_2O_3 was investigated by thermochemical software FactSage®, represented in figure 6. It shows a difference from what has been described to date [13]. In all phase diagrams of the above mentioned compounds published in different literature, a miscibility gap can be observed in the region between CaF_2 and Al_2O_3.

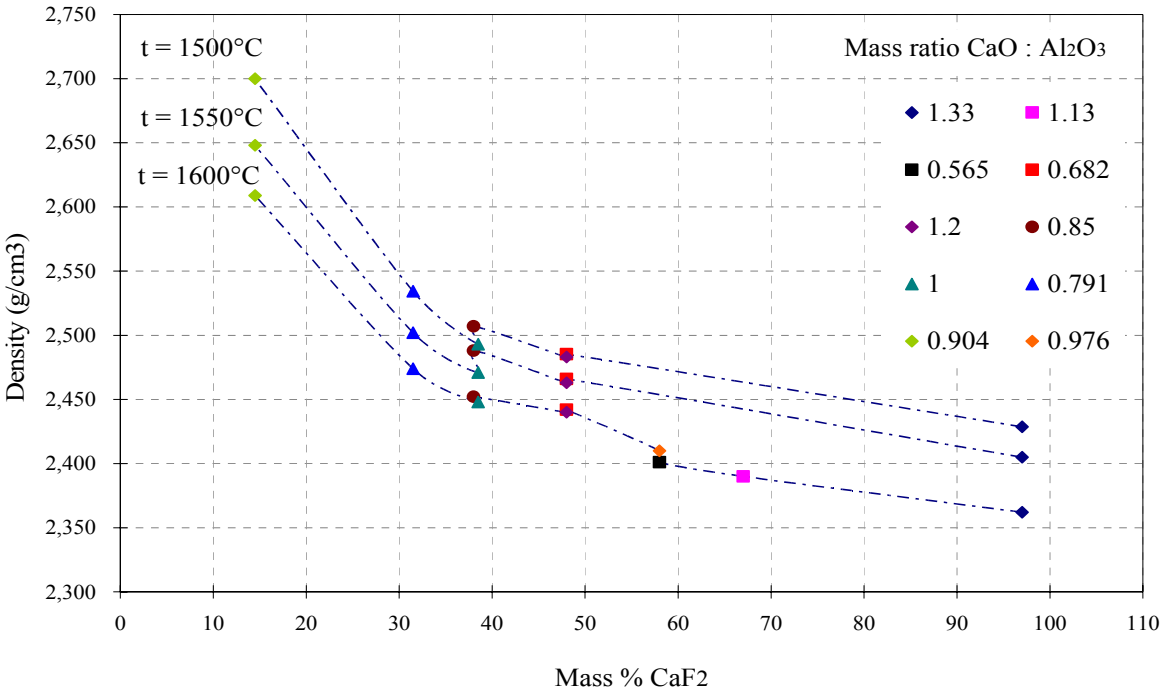

Figure 4: Densities of ESR fluxes with increasing CaF_2 content at different temperatures

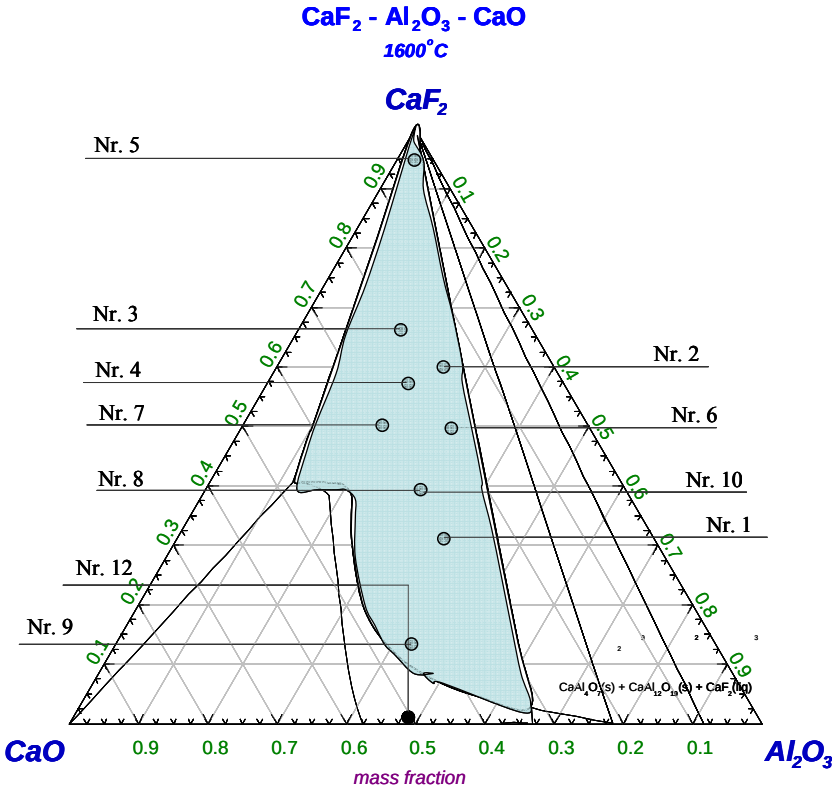

Figure 5: New ternary phase diagram of CaF_2-CaO-Al_2O_3 modelled by FactSage®

Our FactSage® -calculated phase diagram based on SLAGA solution phase modelling system (see fig. 5) shows this miscibility gap more expanded than that of the literature [13]. This phase can only incorporate a certain amount of CaF_2 depending on the respective oxide composition. Excess CaF_2 will be found in the calculation as a separate liquid phase. Therefore, this miscibility gap divides an electroflux melt into two molten phases: slag $_{(L)}$ and $CaF_{2\,(L)}$. From the ternary diagram it can be derived that most of the electrofluxes investigated in this paper are located in the miscibility gap area. This second effect, which can influence the results of the highly sensitive experiments, can be named as the second reason for some differences in the findings.

An exemplary analysis of electroflux Nr. 1 via Scanning Electron Microscopy (SEM), proved the theory of a two-phase area as well as the existence of third (solid) phases. This SEM pattern shows three different phases in this material; a basic phase (matrix), a dark emplacement as well as some crystal-like grains. The SEM Pattern as well as a solidified flux block after experiment has been illustrated in Figure 6. Three EDX-diagrams (figure 7) prove also the presence of these three phases, showing a dark phase containing mostly Calcium, Graphite as well as oxygen. It can be assumed that this phase is due to the partially dissolution of glassy carbon crucible. The crystalline phase contains mostly Calcium and Oxygen, so CaO- and /or CaO-containing phases represent this part (see fig. 7 left). This phase might be attributed to the minor Slag $_{(L)}$ phase in the ternary phase diagram of CaF_2-CaO-Al_2O_3. Furthermore, the matrix, shown in the centre of figure 7 contains mostly Calcium, Fluorine and Oxygen, representing $CaF_{2\,(L)}$ as the major phase.

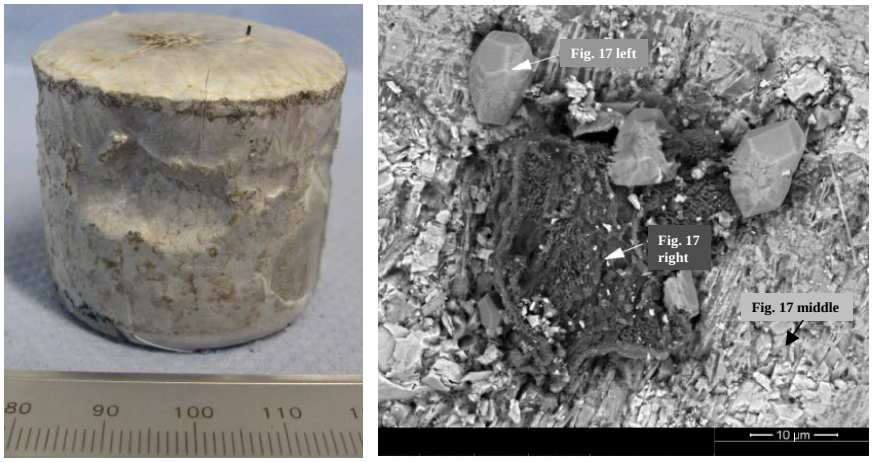

Figure 6: Solidified electroflux after experiment (left) and a SEM-pattern of electroflux Nr. 1 showing three different phases (right)

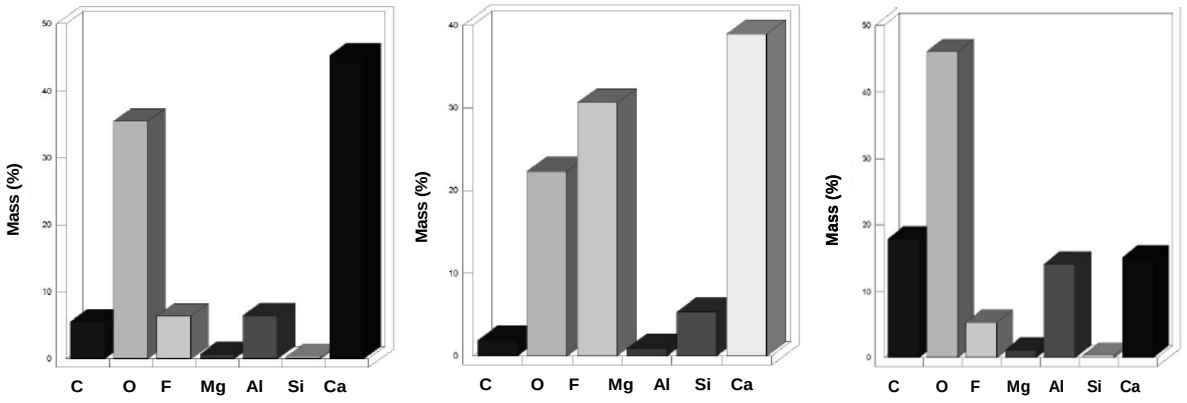

Figure 7: EDX analysis of three phases found in a solidified cross section of Flux Nr. 1; from left to right crystalline-like grain, matrix and dark phase (refer to fig. 6)

The accuracy of the results is illustrated in figure 8 exemplary for two electrofluxes, whose density measurements have been repeated showing an improvement in standard deviation of the results. Furthermore, the chemical compositions of electrofluxes after measurements have not been changed significantly due to the established experimental chamber, in which the evaporation of electrofluxes contents – especially fluorspar – was significantly minimized as well as the interaction with remaining air components.

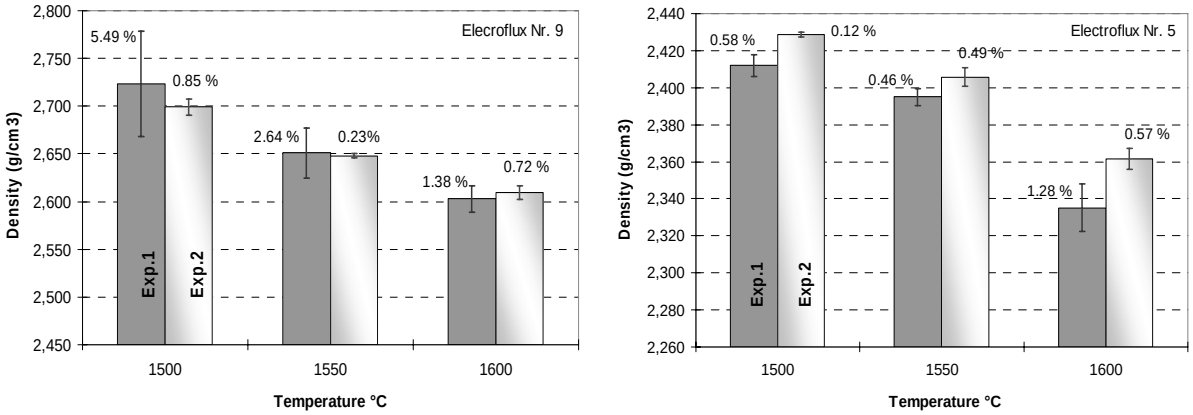

Figure 8: Electrofluxes Nr. 9 (left) and 5 (right), showing an improvement in standard deviation of results after repetition of density experiments

Conclusion

For commonly applied ESR Electrofluxes in the system CaF_2-CaO-Al_2O_3, the density has been investigated as a function of temperature and CaF_2 content, based on the Archimedes method. Measurements are supported by FactSage® calculations. A liquid phase appears to be physically present at roughly 1050°C, yet, this phase represents < 10% of the total system mass. At roughly 1250°C, when a $Ca_3MgAl_4O_{10}$ phase melts, the mass fraction can approach 50% of the total system. At 1414°C excess solid CaF_2 melts and results in system of more than 90% liquid fraction, which appears to be liquid from a practical point of view, yet a fraction of <10 wt% $Ca_5Ti_4O_{13}$ seem to be stable up to 1800°C.

The experimental density results show the expected order with rising values of calcium fluoride. Fluxes containing similar amounts of CaF_2 have density values rather close to each other, although the mass ratios of CaO:Al_2O_3 are different. The possibility of existing "not-melted" particles even up to 1600-1800°C can lead to uncertainties in the measurements. A phase diagram has been optimized and shows that most of the electrofluxes investigated are located in a miscibility gap area and the density measurement can not be assured to be in Slag $_{(L)}$ or in a $CaF_{2\,(L)}$ phase. That could also falsify the results of the highly sensitive experiments. Nevertheless the accuracy of the results could be proven and the chemical compositions have not been changed considerably due to the used chamber technique.

References

1. M.Wahlster, H.-J. Kingelhoefer, A.Choudhury, "A contribution to metallurgy and technology of ESR-Process", Proceeding ICSTIS, Section2, 1970, pp.327-331;
2. K. M. Kelkar, S. V. Patankar, "Computational Modeling of the Electroslag Remelting (ESR) Process", LMPC Conference, 2005, pp.1-8;
3. G. E. Totten, Steel Heat Treatment, CRC Press, 2006, P. 661
4. Nat. Res. Coun., (U.S.). Comm. on Electroslag Remelting and Plasma Arc Melting Edition, Electroslag Remelting and Plasma Arc Melting, National Academy of Sciences, 1976, pp. 25-27;

5. C. K. Gupta, Chem. metallurgy: principles and practice, Wiley-VCH Publisher, 2003, p 435;
6. S. Akbari, B. Friedrich, “Challenges in Measuring of Physical Properties of Liquid Phases for Materials and Process Optimization”, Advanced Eng. Mat., Vol. 9, No. 4, 2007, pp. 280-28
7. E.R. Van Artsdalen, I.S. Yaffe, “ Electrical conductivity and density of molten salt systems: KCl-LiCl, KCl- NaCl and KCl-KI”, 1955, Vol. 59, pp. 118-127
8. K. Arndt, A. Geßler, “ Dichte und Äquivalentleitfähigkeit einiger geschmolzener Salze”, Zeitschrift für Elektrochemie, 1933, Nr. 39, pp. 665-667
9. A.D. Kirshenbaum, et al., “Density of liquid NaCl and KCl and an estimate of their critical constants together with those of the other alkali halides”, J. Inorg.Nucl. Chem., 1962, Vol. 24, pp. 1287-1296
10. M.F. Driza, Properties of Elements, Moscow Publishing House Library, Russian Article, 2003, P.66
11. Ogino, K.; Hara, S., “Density, surface tension and elecrticla conductivity of calcium fluoride based fluxes for electroslag remelting”, Iron and Steel Institute of Japan (ISIJ), Japanese Journal, Vol. 63, 1977, P. 2141
12. Slag Atlas, Edited by Verein Deutscher Eisenhüttenleute (VDEh), Verlag Staheisen GmbH, Düsseldorf, 1995, P. 327
13. B. Sikora and M. Zielinski, “Density, Surface Tension, Viscosity and Electrical Conductivity of Fused Calcium Oxide-Alumina-Calcium Fluoride Systems,” Hutnik, Vol. 41, Nr. 9, 1974, pp. 433-437